Evaluation of Liquefaction Hazard in the West Coastal Area of Bengkulu City Due to Megathrust Earthquake

Fitria Leonni Valetta, Lindung Zalbuin Mase*, Khairul Amri, Rena Misliniyati, & Hardiansyah
Department of Civil Engineering, University of Bengkulu, Indonesia
*Corresponding Author: G1B021027.fitrialeonnivaletta@mhs.unib.ac.id

Received: 17th May 2025; **Accepted**: 25th July 2025; **Published**: 30th July 2025
DOI: https://dx.doi.org/10.29303/jpft.v11i1a.9070

Abstract - *This study analyzes the liquefaction potential in the coastal area of Bengkulu due to the large subduction earthquake in 2007. The study was conducted systematically, beginning with field investigations with shear wave velocity measurements. Spectral matching and ground motion prediction based on relative attenuation models were conducted to obtain a representative picture of ground motion at the study site. Subsequently, soil response analysis was used to evaluate the behaviour of the soil under seismic loading. A non-linear finite element approach was applied to assess the dynamic characteristics of the soil, including excess pore water pressure, shear stress-strain response, and stress path. In addition, an empirical evaluation was conducted to determine the liquefaction potential. The results show that liquefaction has the potential to occur at shallow depths, especially in the first and second layers of the sand layer. The results of numerical and empirical analyses show consistent patterns and agreement. The comparison between the excess pore pressure ratio and the safety factor aligns with the findings from previous studies. These findings emphasise the importance of implementing seismic hazard mitigation measures in the study area.*

Keywords*: liquefaction, Ground response, Non-linear analysis, Peak ground acceleration*

INTRODUCTION

Bengkulu Province, located on the seismically active Sumatra belt, has unique characteristics of earthquake activity in Indonesia. The region has been the epicentre of some of the largest earthquakes over the past 20 years, with Bengkulu Province recorded to have experienced two major shocks, one of which occurred on 12 September 2007 with a magnitude of M_w 8,6. The 2007 earthquake and its seismic impacts caused liquefaction, particularly in the Lempuing and Tanah Patah areas of Bengkulu City (Mase, 2024). Liquefaction, a phenomenon in which soil loses strength and changes from solid to liquid, is significant in causing damage. The impacts include subsidence, the appearance of cracks, and lateral movement of soil. (Mase, Tanapalungkorn, et al., 2022a).

Bengkulu Province is located near several active earthquake sources, including three primary sources, namely the Sumatra Subduction Zone, the Mentawai Fault, and the Sumatra Fault (Mase, 2020). The impact of these three earthquake sources has resulted in earthquake disasters in the coastal and mountainous areas of Sumatra Island. Bengkulu Province, which is located close to these earthquake sources, often experiences a high level of seismic vulnerability (Misliniyati et al., 2018). Figure 1 shows the tectonic map of Bengkulu Province.

Previous studies have generally focused on understanding earthquake characteristics and investigating the vulnerability of ground damage during earthquakes. Misliniyati et al. (2013) investigated the potential for earthquake-induced liquefaction in one of the coastal areas of Bengkulu City. The results showed that the soil in the area is dominated by sand and is highly susceptible to liquefaction at shallow depths. Mase (2018) examined the seismic response of soils in the coastal area of Bengkulu using the M_w 8,6 earthquake

waves that occurred in September 2007 and compared it with the seismic design of the Indonesian design code SNI-1726-2019. The results show that the seismic waves at the surface tend to exceed the existing seismic design in Bengkulu City. Mase dkk. (2024) investigated the bedrock depth along the downstream segment of Muara Bangkahulu River, Bengkulu City. Bedrock information is helpful for simulating seismic response analyses of soils. Thus, research on the seismic response of the ground during the Megathrust Earthquake in the South Coastal area of Bengkulu Province has not been conducted. However, a rough interpretation of the earthquake's impact has been achieved.

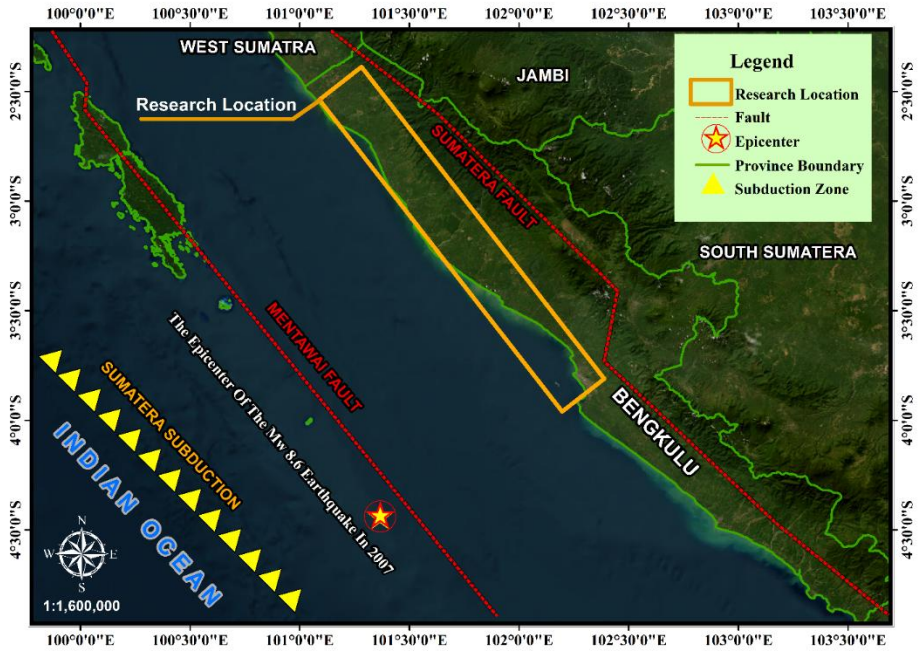

Figure 1. Tectonic condition map of Bengkulu Province (modified from Mase 2020)

RESEARCH METHODS

Study Area and Site Investigation Results

The study focussed on several locations along the Bengkulu coastline mapped in Figure 2, which are marked with yellow dots on the study map. Each site was labelled PB (Pantai Bengkulu), followed by 1-14, indicating the order of observation points. Of these, six main sites, PB-1, PB-4, PB-5, and PB-8, were selected to represent the general geological conditions in the area. These sites include Muko-Muko, Air Muring, Ketahun, and Bengkulu; as shown in Figure 3, sandy material dominates the soil composition in these areas. Some sites, such as PB-4 and PB-5, consist almost entirely of sand, while thin clay layers appear in PB-1 and PB-8. In line with NEHRP, the site class in coastal Bengkulu province also belongs to Site Class D (180 m/s $\leq V_{s30} <$ 360 m/s), with V_{S30} values (mean shear wave velocity at 30 m depth) ranging from 191 to 626 m/s.

One-Dimensional Seismic Response Analysis

The input parameters are soil layer data, shear wave velocity (V_s) profiles, and earthquake wave data. Investigation of soil behaviour during the M_w 8.6 earthquake used one-dimensional soil seismic response analysis. An illustration of the soil seismic response model for the South Coastal region of Bengkulu Province is presented in Figure 3. The one-dimensional soil framework used in this study was developed based on research conducted by Pender et al. (2016) dan Mase et al. (2019). The finite element

method was used to simulate the soil response analysis. The soil profile mesh was obtained based on the wavelength analysis suggested by Mase et al. (2022). All soil layers should have a minimum frequency (f) of 30 Hz (Hashash et al., 2015). Thus, the mesh derivative can be obtained using the assumptions shown in Equation 1

$$d = \frac{V_S}{4f_{max}} \quad (1)$$

Where d: mesh size; $f_{(max)}$: maximum frequency used is 30 H_z. V_s: shear wave velocity (m/s) (Hashash et al., 2015).

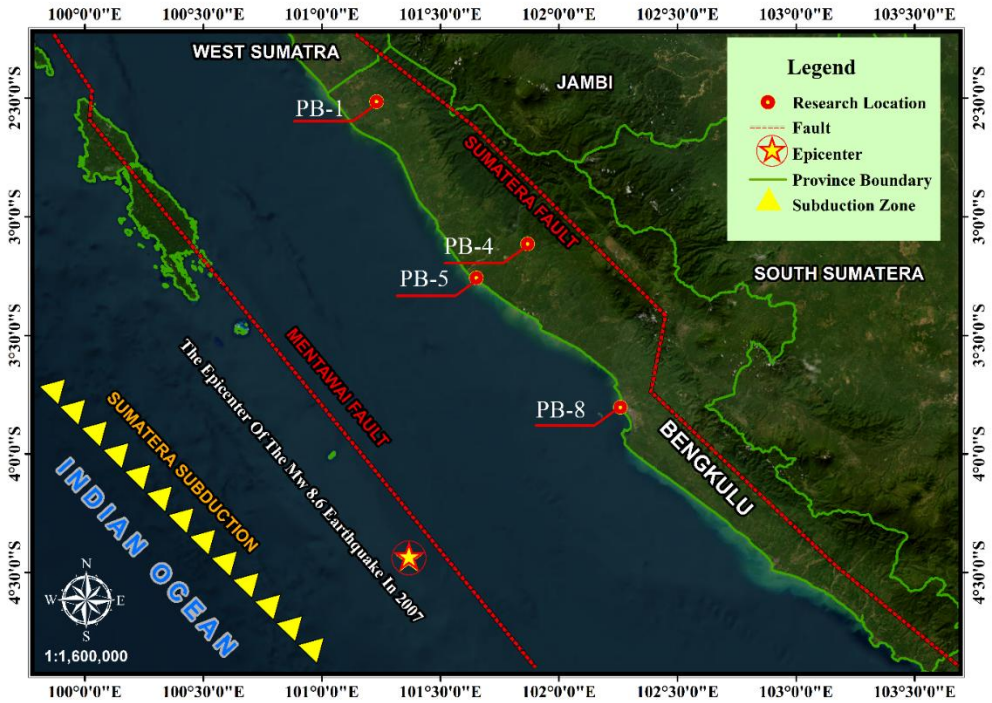

Figure 2. Research location map (modified *Google Earth*, 2025

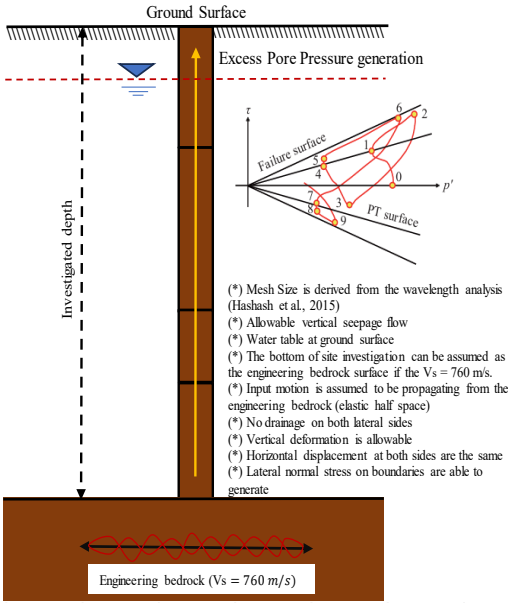

Figure 3. Seismic soil response analysis scheme (adaptation Zalbuin Mase et al. 2025)

Spectral Matching Method

This study will examine the ground response following the most significant megathrust earthquake in Bengkulu City, the Bengkulu-Mentawai Earthquake, with a magnitude of M_w 8,6 in 2007. Figure 4 displays the spectral acceleration at the study site predicted using the model of Idini et al. (2017). In the figure, the peak ground acceleration (PGA) varies from 0.103 to 0.154g. At PB-1 (Figure 4a), the PGA value is about 0.103g, while at PB-4 (Figure 4b), it shows a value of 0.148g. At PB-5 (Figure 4c) and PB-8 (Figure 4d), the PGA values are 0.151g and 0.154g, respectively. Regarding spectral acceleration, the maximum values generally occur in the 0.15 to 0.5 seconds. Based on predictions using the model of

Idini et al. (2017), the peak spectral acceleration ranges from 0.538 to 1.374g.

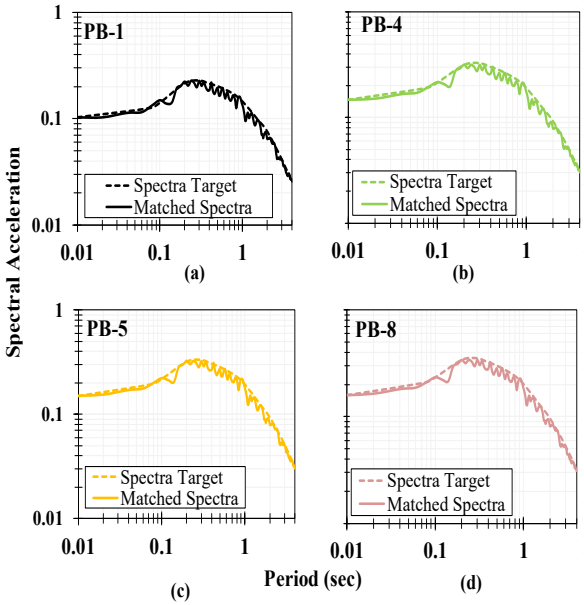

Figure 4. Spectral matching for the observed Sites. (a) PB-1, (b) PB-4, (c) PB-5 and (d) PB-8.

The ground motions at the site are generated from the corresponding spectral accelerations, as presented in the figure. From the figure, the peak ground acceleration at the surface ranges from 0.0929 g to 0.1357 g; for PB-1 (figure 7a), the PGA is about 0.1357g. for PB-4 (figure 7b), the PGA is about 0.1084g. for PB-5 and PB-8 (figure 7e), the PGA is about 0.0929g. The spectral matching results show good consistency. Based on the study of Mase dkk. (2023), the PGA values are within the range of 0.0892 to 0.1542g, so the predictions obtained from previous studies are generally based on the findings in this study. In addition, the resulting ground motion patterns showed similarities with the estimated ground motions during the earthquake event. The ground motion results were then used as input in the ground response analysis.

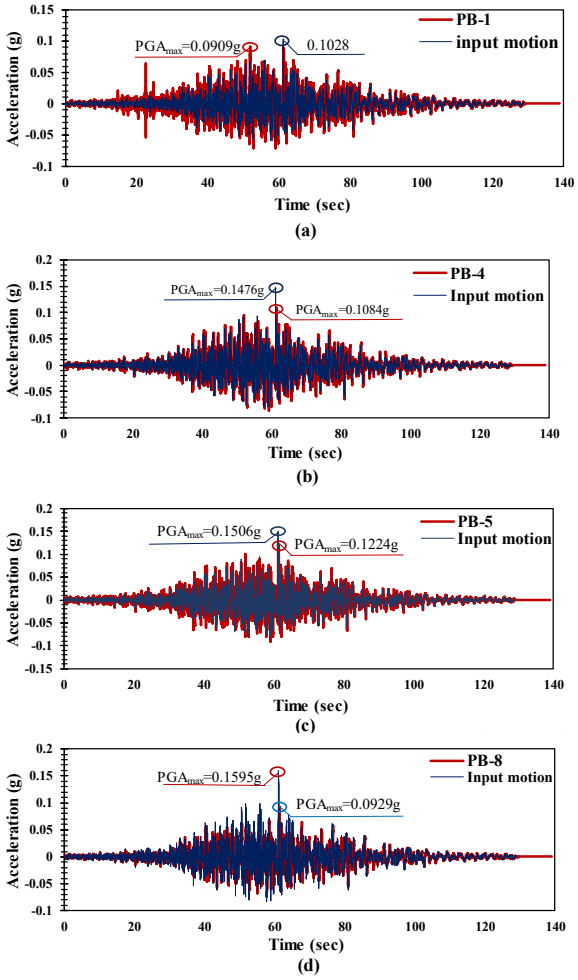

Figure 5. The ground motion generated from the spectral matching method for Sites (a) PB-1, (b) PB-4, (c) PB-5 and (d) PB-8.

RESULTS AND DISCUSSION

Maximum Acceleration Profile

The maximum acceleration profile obtained from seismic wave propagation is presented in Figure. 6. Figure. 6 shows that the peak ground acceleration propagated by the engineered bedrock generally decreases at the surface. For PB-1 (Figure. 6a), the maximum at the surface of the engineered bedrock, which is 0.146g, decreases to 0.048g. For PB-4 (Figure. 6b), the maximum value at the ground surface varies from 0.111 peak ground acceleration, and this maximum tends to decrease to 0.071g. For PB-5 (Figure. 6c), the maximum value at the ground level is 0.123g, which decreases to 0.068g. For PB-8 (Figure. 6d), the maximum value at ground level is 0.114g, decreasing

to 0.09g. Dammala et al. (2019) stated that strong input motions can result in de-amplification at shallow depths. The reduction of peak ground acceleration in non-linear analyses may occur because the ground response is no longer linear (Kawan et al. 2022). Therefore, the hysteretic loop is not in a linear response anymore. This indicates that the shear strength of the soil has reached the linear limit.

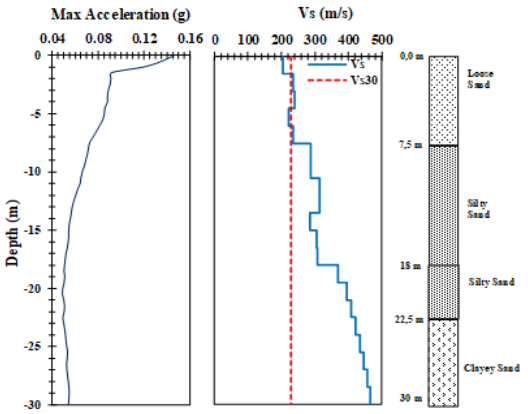

(a)

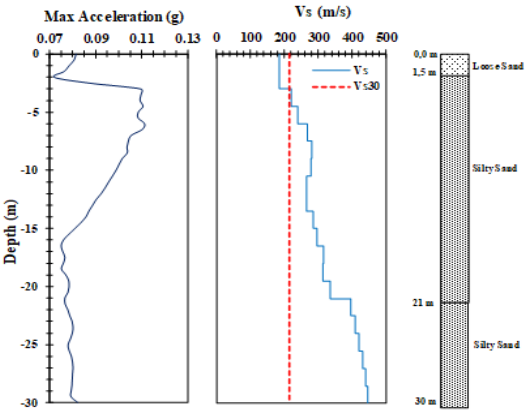

(b)

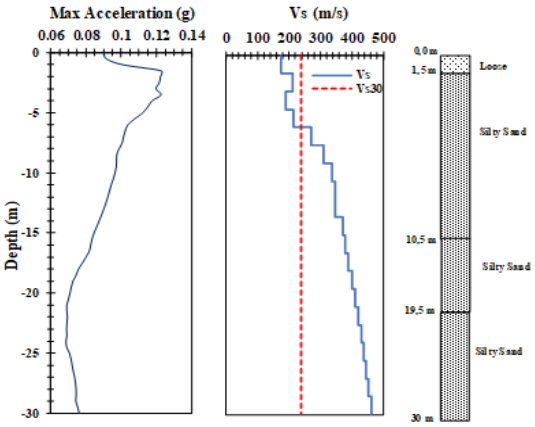

(c)

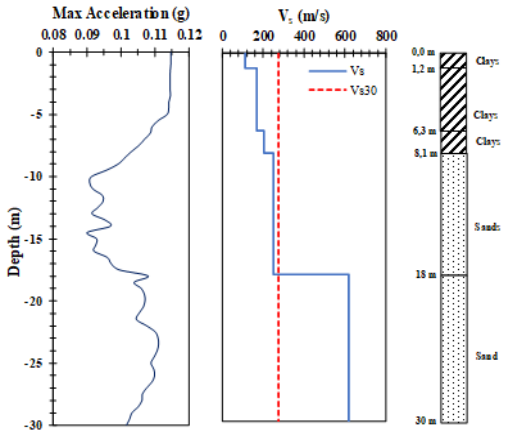

(d)

Figure 6. ground accelerations associated with Vs for Sites (a) PB-1, (b) PB-4, (c) PB-5 and (d) PB-8.

Respons Spektral Akselerasi

In Figure. 7, a comparison is made for the input and surface spectral accelerations. Two spectral accelerations are compared to observe the frequency trend during seismic wave propagation. Figure 7 also presents the two spectral accelerations designed for the three main site classes in the study area, namely soft soil or Site Class E, medium soil or Site Class D and stiff soil or Site Class C, from the Indonesian seismic code or SNI 1726 2019. The inputted spectral acceleration (blue line) does not exceed the designed design, especially at PB-1 (Figure. 7a), PB-4 (Figure. 7b), PB-5 (Figure. 7c), and PB-8 (Figure. 7d). Generally, the peak spectral acceleration of the input motion occurs at a period of 0.2 to 0.5 s, with the peak value varying from 0.207g to 0.425g. The period range (0.2 to 0.5 s) shows the resonance of acceleration at low periods. According to Mase et al. (2021), low to medium periods indicate low to medium-rise buildings. Mase et al. (2021) also revealed that damage to structural buildings can be significant when resonance between the seismic wave motion period and the building structure occurs. Hausler E & Anderson A (2007) stated that low- to medium-rise buildings in Bengkulu City could experience

significant impacts in 2007. In line with previous studies and this research, damage from earthquake shaking can be significant in low- and medium-rise buildings.

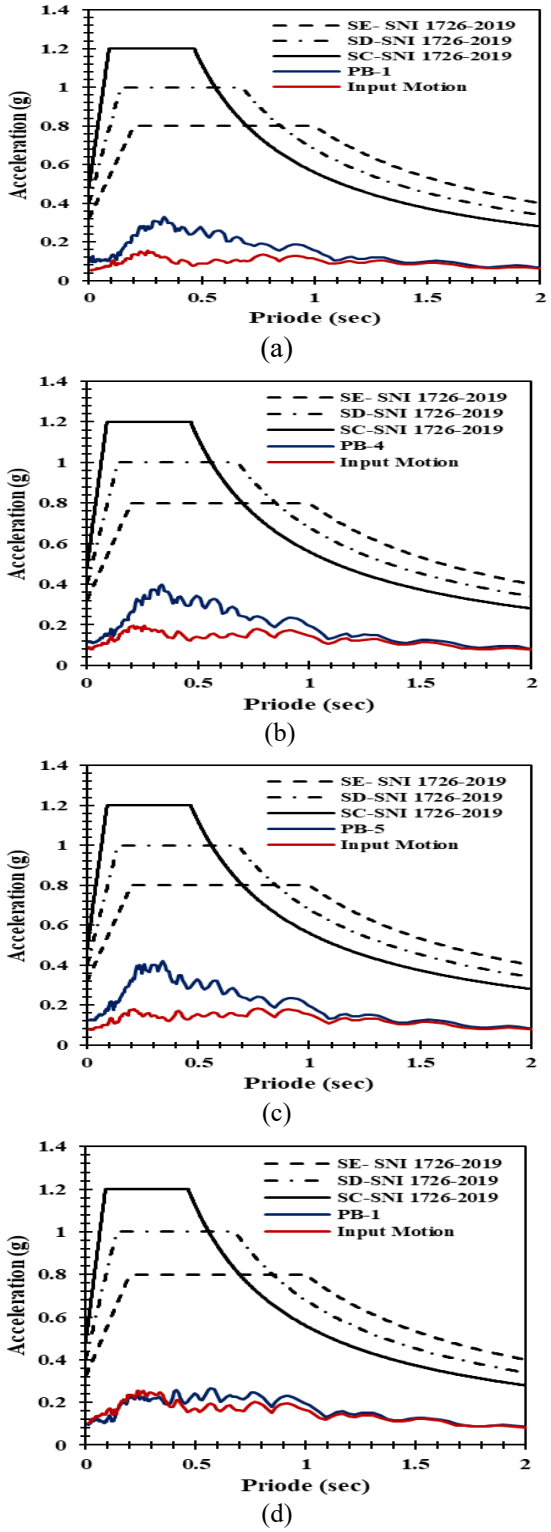

Figure 7. Comparison of nonlinear acceleration spectra response and input waves

Figure 7 also presents the surface spectral accelerations for each studied site. The spectral acceleration at the ground surface is generally lower than the input motion and the designed spectral acceleration. The peak spectral accelerations at sites PB-1 (Figure. 7a), PB-4 (Figure. 7b), PB-5 (Figure. 7c), and PB-8 (Figure. 7d) are generally shifted to the higher frequency (short period) side. According to Yefei dkk. (2013), the change in the trend of spectral acceleration at the ground surface indicates that the nonlinearity of the soil plays an important role. This study's change in spectral acceleration trends from bedrock to near-surface layers initially occurred at shallow depths, especially for layers with low shear resistance. Yoshida (2015) mentioned that the soil's nonlinearity affects the soil's response during strong movements.

Weak layers with low shear resistance are generally found at shallow depths in the study area. Sandy layers having Vs of about 173 to 461 m/s are generally found from 30 m to the ground surface. This trend is also predicted to occur at depths in this range. In other words, weak soil layers at this depth range can significantly affect soil behaviour. Affect soil behaviour. This depth range was predicted to experience liquefaction in 2007. Furthermore, the response of the soil during seismic wave propagation is presented below.

Pressure Profile and Indication of Liquefaction

Figure 8 compares the excess pore pressure and effective stress. It can be observed that the excess pore pressure exceeds the effective stress at shallow depths, which is about 0.2 to 15 m below the ground surface. Sukkarak et al. (2021) state that liquefaction can occur if the excess pore pressure ratio exceeds the effective stress. For PB-1, PB-4 and PB-5, liquefaction can

occur in the first layer (Figure. 8a, 8b and 8c). For PB-8, the difference between excess pore pressure and effective stress is relatively small for deeper depths (up to 15 m). It can be observed that shallow sandy soils have liquefaction potential. Regarding soil type, classified sandy soil is expected to experience liquefaction. The soil resistance represented by V_s in this layer and the soil type in the study area indicate a weak layer. Generally, the layers suspected of liquefaction in the study area have shear wave velocities ranging from 173 to 250 m/s.

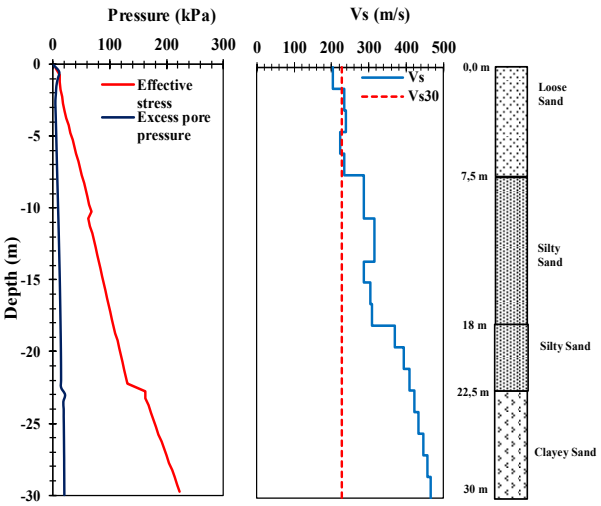

(a)

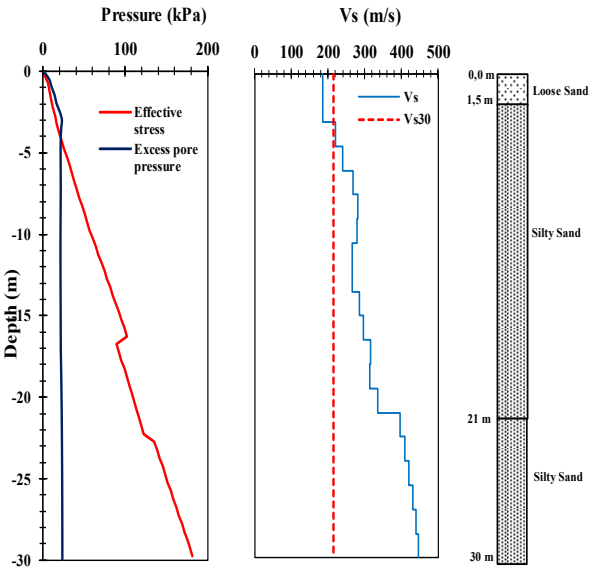

(b)

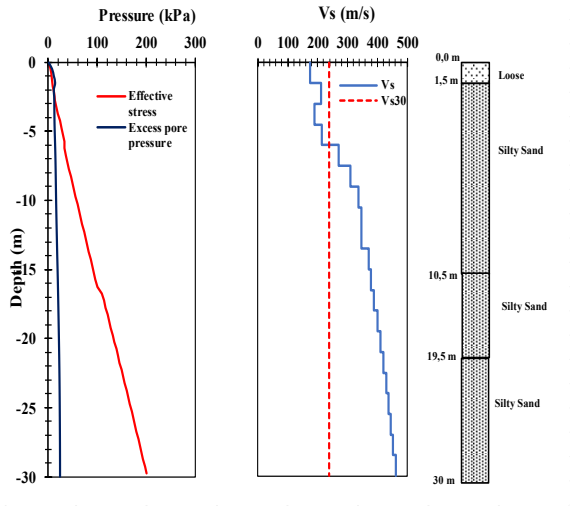

(c)

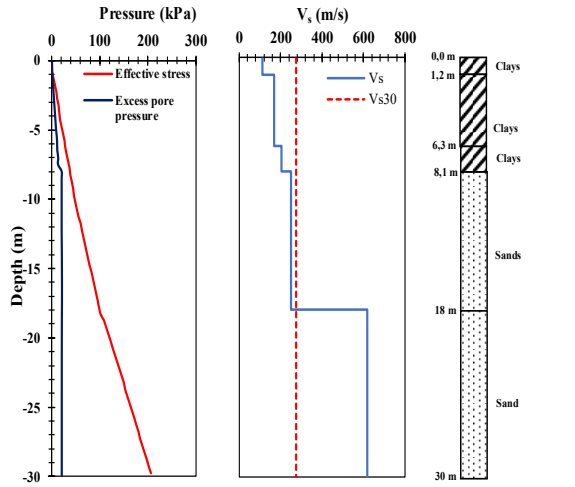

(d)

Figure 8. Excess pore pressure and effective stress with depth for (a) PB-1, (b) PB-4, (c) PB-5 and (d) PB-8.

Excess Pore Pressure

In Figures 9, 10, 11 and 12 the time history of the excess pore pressure ratio clearly shows the occurrence of liquefaction. The figures show that the excess pore pressure ratio exceeds the threshold, indicating liquefaction. In addition, the time histories also show that liquefaction generally occurs starting after 42 to 80 seconds of seismic wave propagation. In PB-1 (Figure. 9a), liquefaction generally occurred after 63 seconds of seismic wave propagation. For PB-4, liquefaction occurred after 42 seconds of seismic wave

propagation. In PB-5, liquefaction occurs after 64 seconds of seismic wave propagation. For PB-8 (Figure. 12a), liquefaction initially occurs after 1 minute. This event illustrates the importance of excess pore pressure in predicting liquefaction, thus improving our understanding of seismic events.

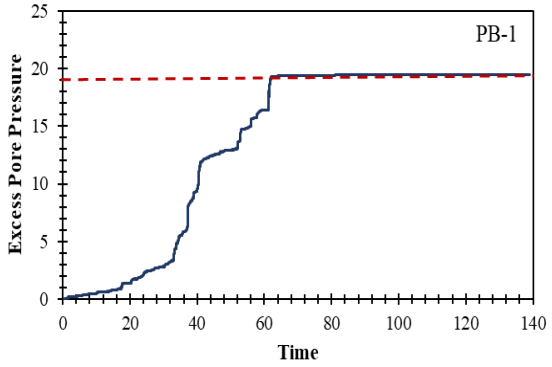

(a)

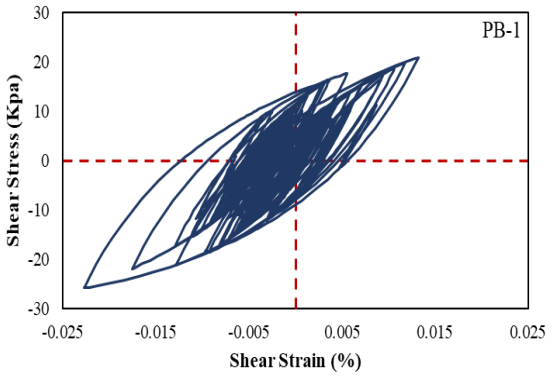

(b)

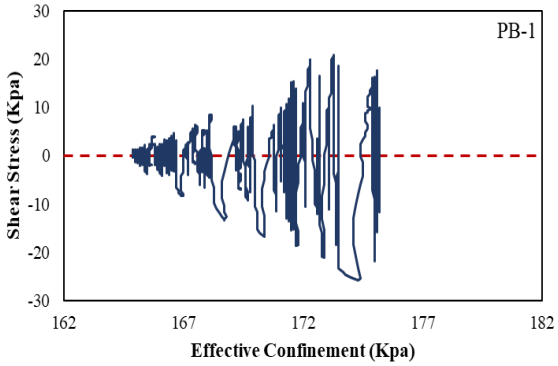

(c)

Figure 9. Dynamic behaviour of the liquid layer for PB-1 at a depth of 24 m.

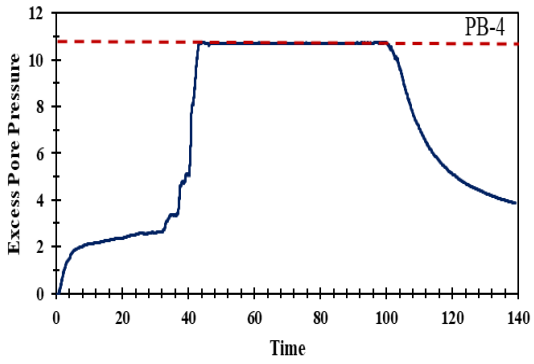

(a)

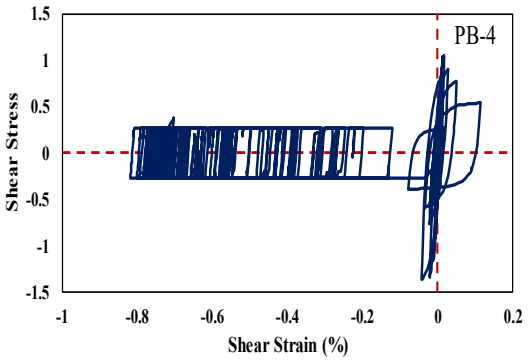

(b)

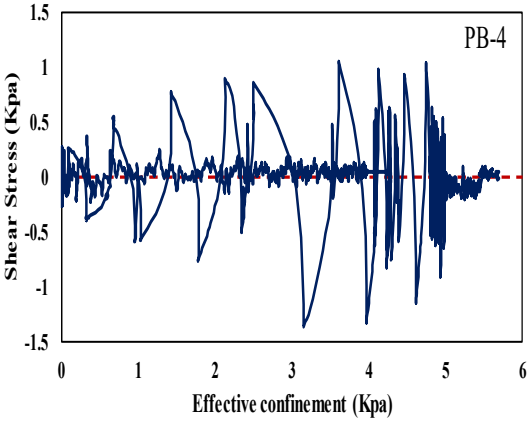

(c)

Figure 10. Dynamic behavior of the liquid layer for PB-4 at 15 m depth.

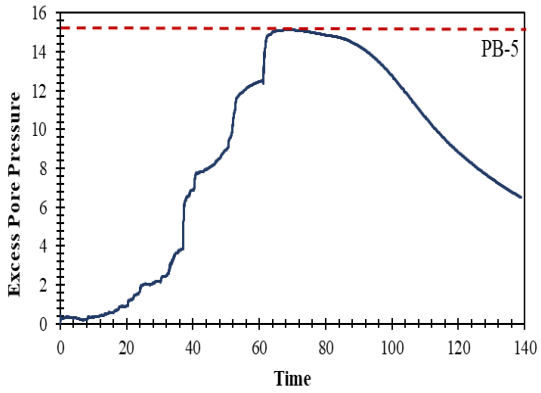

(a)

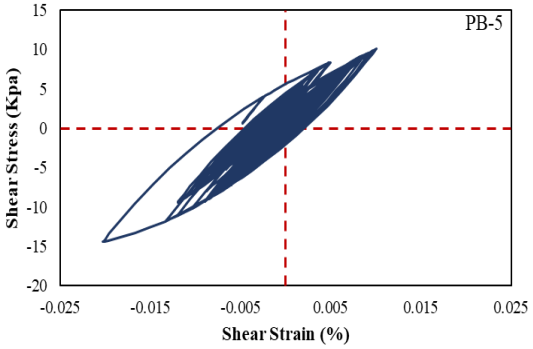

(b)

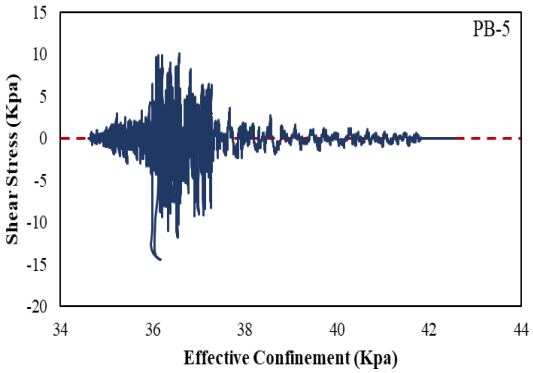

(c)

Figure 11. Dynamic behavior of liquid layer for PB-5 at 8 m depth.

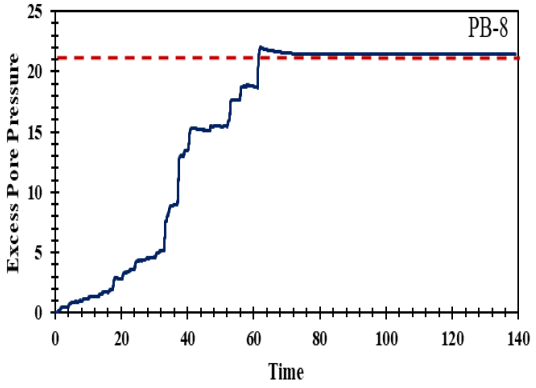

(a)

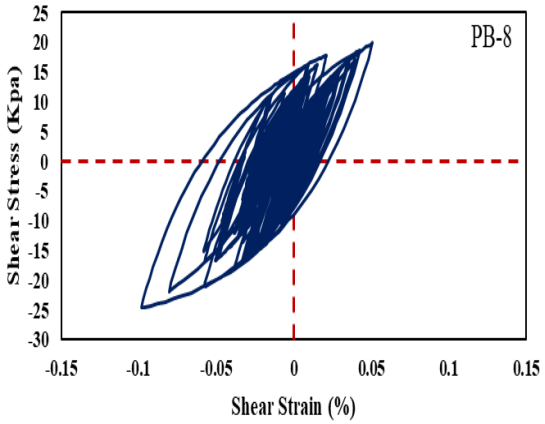

(b)

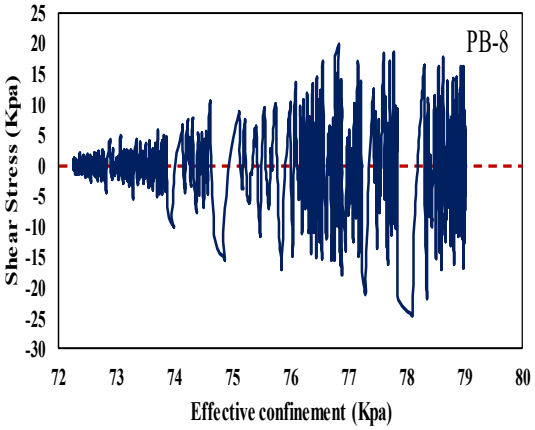

(c)

Figure 12. Dynamic behavior of liquid layer for PB-8 at 15 m depth.

The time history also shows the dissipation of liquefaction pore pressure or the end of liquefaction. It should be noted that soil behaviour is still observed 10 seconds after seismic wave propagation. Therefore, there is an additional 10 seconds of measurement time after the end of seismic wave propagation. Initial pore pressure dissipation may occur at 77 second to 140 second. For PB-1 (Figure. 9a) and PB-8 Figure 12a), the initial time of pore pressure dissipation occurs at the 140 second. For other locations, the initial time of pore pressure dissipation occurs at the 103 second for PB-4 (Figure. 10a) and 77 second for PB-5 (Figure 11a). In line with the prediction of the onset of liquefaction, it can be predicted that the duration of liquefaction in the 2007

Bengkulu-Mentawai Earthquake ranged from 84 to 138 seconds.

Shear Stress and Shear Strain Curves

Figures 9b, 10b, 11b and 12b display the shear stress versus shear strain curves (hysteretic loops) at the depths studied. From the visualisation, there is an inconsistent pattern in the hysteretic loop, which reflects the non-linear behaviour of the soil. The curve's flattening in this loop indicates a decrease in shear modulus (Khosravi et al., 2018). The shear modulus is a dynamic parameter influenced by effective stress (Sas et al., 2015). The decrease in modulus implies a decrease in effective stress. Thus, a significantly reduced shear modulus can reflect a weakening of the effective stress (Zhou et al., 2017). The decrease in effective stress is directly related to the increase in excess pore pressure. During the liquefaction process in sandy soils, the pore pressure increases, causing the effective stress to decrease. This effective stress is closely related to the shear resistance of the soil. When the sandy soil loses its strength, the failure of the soil structure is accompanied by a non-linear response. Therefore, the liquefied soil layer shows a marked decrease in shear modulus. The pattern in the hysteretic circle confirms the indication of liquefaction in the sandy soil at the study site.

Effective Stress Path

As shown in Figures 9c, 10c, 11c and 12c the dots representing each study site indicate that the effective stress path plays an important role in understanding the ground settlement potential. It is observed that the adequate restraint pressure decreases to zero during the seismic wave, which causes an increase in excess pore pressure and a sufficient decrease in restraint pressure. When the adequate confining pressure reaches zero, this condition leads to a loss of bearing capacity of the soil. The loss of bearing capacity indicates that the soil can no longer support the load, which can result in the sinking of the structure during a liquefaction event

CONCLUSION

This paper discusses the liquefaction potential in the coastal province of Bengkulu through ground motion prediction, spectral matching, and soil response analysis. From the results, several conclusions can be drawn.

1. The analysis results show that sandy soils dominate the study area. Sandy soils with Vs < 180 m/s near the surface have the potential to experience liquefaction due to the 2007 Bengkulu-Mentawai Earthquake. In addition, subsidence can occur in sandy soils.
2. The spectral acceleration resulting from seismic soil response analysis does not exceed the spectral acceleration design value of SNI-1726-2019. It predominantly occurs at short periods, indicating resonance with low—to medium-rise structures.
3. Analysis of liquefaction potential indicates that the top two layers of sand are at risk of liquefaction during an earthquake. In general, the results of this study describe the environmental conditions in the study area, which are helpful as recommendations for local governments in developing earthquake mitigation-based spatial plans in Bengkulu.

REFERENCES

Dammala, P. K., Kumar, S. S., Krishna, A. M., & Bhattacharya, S. (2019). Dynamic soil properties and liquefaction potential of northeast Indian soil for non-linear effective

stress analysis. *Bulletin of Earthquake Engineering*, *17*(6), 2899–2933. https://doi.org/10.1007/s10518-019-00592-6

Hashash, Y. M. A., Dashti, S., Romero, M. I., Ghayoomi, M., & Musgrove, M. (2015). Evaluation of 1-D seismic site response modeling of sand using centrifuge experiments. *Soil Dynamics and Earthquake Engineering*, *78*, 19–31. https://doi.org/10.1016/j.soildyn.2015.07.003

Hausler E, & Anderson A. (2007). *Observation of the 12 and 13 September 2007Earthquake, Sumatra, Indonesia.*

Idini, B., Rojas, F., Ruiz, S., & Pastén, C. (2017). Ground motion prediction equations for the Chilean subduction zone. *Bulletin of Earthquake Engineering*, *15*(5), 1853–1880. https://doi.org/10.1007/s10518-016-0050-1

Khosravi, A., Shahbazan, P., & Pak, A. (2018). Impact of hydraulic hysteresis on the small strain shear modulus of unsaturated sand. *Soils and Foundations*, *58*(2), 344–354. https://doi.org/10.1016/j.sandf.2018.02.018

Mase, L. Z. (2018). Reliability study of spectral acceleration designs against earthquakes in Bengkulu City, Indonesia. *International Journal of Technology*, *9*(5), 910–924. https://doi.org/10.14716/ijtech.v9i5.621

Mase, L. Z. (2020). Seismic Hazard Vulnerability of Bengkulu City, Indonesia, Based on Deterministic Seismic Hazard Analysis. *Geotechnical and Geological Engineering*, *38*(5), 5433–5455. https://doi.org/10.1007/s10706-020-01375-6

Mase, L. Z. (2024). A Case Study of Liquefaction Potential Verification During a Strong Earthquake at Lempuing Subdistrict, Bengkulu City, Indonesia. *Transportation Infrastructure Geotechnology*, *11*(4), 1547–1572. https://doi.org/10.1007/s40515-023-00335-w

Mase, L. Z., Likitlersuang, S., & Tobita, T. (2019). Cyclic behaviour and liquefaction resistance of Izumio sands in Osaka, Japan. *Marine Georesources and Geotechnology*, *37*(7), 765–774. https://doi.org/10.1080/1064119X.2018.1485793

Mase, L. Z., Likitlersuang, S., & Tobita, T. (2021). Ground Motion Parameters and Resonance Effect During Strong Earthquake in Northern Thailand. *Geotechnical and Geological Engineering*, *39*(3), 2207–2219. https://doi.org/10.1007/s10706-020-01619-5

Mase, L. Z., Likitlersuang, S., & Tobita, T. (2022). Verification of Liquefaction Potential during the Strong Earthquake at the Border of Thailand-Myanmar. *Journal of Earthquake Engineering*, *26*(4), 2023–2050. https://doi.org/10.1080/13632469.2020.1751346

Mase, L. Z., Tanapalungkorn, W., Likitlersuang, S., Ueda, K., & Tobita, T. (2022). Liquefaction analysis of Izumio sands under variation of ground motions during strong earthquake in Osaka, Japan. *Soils and Foundations*, *62*(5). https://doi.org/10.1016/j.sandf.2022.101218

Misliniyati, R., Mase, L. Z., Syahbana, A. J., & Soebowo, E. (2018). Seismic hazard mitigation for Bengkulu Coastal area based on site class analysis. *IOP Conference Series: Earth and Environmental Science*, *212*(1). https://doi.org/10.1088/1755-1315/212/1/012004

Misliniyati, R., Razali, M. R., & Muktadir, R. (2013). BERDASARKAN DATA CONE PENETRATION TEST DI

KELURAHAN LEMPUING, KOTA BENGKULU. In *Jurnal Inersia* (Vol. 5, Issue 2).

Pender, M. J., Orense, R. P., Wotherspoon, L. M., & Storie, L. B. (2016). Effect of permeability on the cyclic generation and dissipation of pore pressures in saturated gravel layers. *Geotechnique*, *66*(4), 313–322. https://doi.org/10.1680/jgeot.SIP.15.P.024

Sas, W., Gabryś, K., & Szymański, A. (2015). Effect of time on dynamic shear modulus of selected cohesive soil of one section of express way no. S2 in Warsaw. *Acta Geophysica*, *63*(2), 398–413. https://doi.org/10.2478/s11600-014-0256-z

SNI 1726 2019. (n.d.).

Sukkarak, R., Tanapalungkorn, W., Likitlersuang, S., & Ueda, K. (2021). Liquefaction analysis of sandy soil during strong earthquake in Northern Thailand. *Soils and Foundations*, *61*(5), 1302–1318. https://doi.org/10.1016/j.sandf.2021.07.003

Yoshida, N. (2015). *Geotechnical, Geological and Earthquake Engineering Seismic Ground Response Analysis*. http://www.springer.com/series/6011

Zalbuin Mase, L., Tanapalungkorn, W., Likitlersuang, S., Ueda, K., & Tobita, T. (2025). Ground motion, liquefaction and hazard analysis at the Palu site during the 2018 Indonesian great earthquake. *China Geology*, *8*(0), 1–23. https://doi.org/10.31035/cg20240065

Zhou, W., Chen, Y., Ma, G., Yang, L., & Chang, X. (2017). A modified dynamic shear modulus model for rockfill materials under a wide range of shear strain amplitudes. *Soil Dynamics and Earthquake Engineering*, *92*, 229–238. https://doi.org/10.1016/j.soildyn.2016.10.027